Acta Oceanol. Sin., 2015, Vol. 34, No. 1, P. 73–78
DOI: 10.1007/s13131-015-0599-6
http://www.hyxb.org.cn
E-mail: hyxbe@263.net

Wave height measurement in the Taiwan Strait with a portable high frequency surface wave radar

ZHOU Hao[1,2]*, ROARTY Hugh[3], WEN Biyang[1]

[1] School of Electronic Information, Wuhan University, Wuhan 430072, China
[2] Suzhou Institute of Wuhan University, Suzhou 215123, China
[3] Institute of Marine and Coastal Sciences, Rutgers University, New Jersey 08901, USA

Received 12 December 2013; accepted 23 September 2014

Abstract

As an important equipment for sea state remote sensing, high frequency surface wave radar (HFSWR) has received more and more attention. The conventional method for wave height inversion is based on the ratio of the integration of the second-order spectral continuum to that of the first-order region, where the strong external noise and the incorrect delineation of the first- and second-order Doppler spectral regions due to spectral aliasing are two major sources of errors in the wave height. To account for these factors, two more indices are introduced to the wave height estimation, i.e., the ratio of the maximum power of the second-order continuum to that of the Bragg spectral region (RSCB) and the ratio of the power of the second harmonic peak to that of the Bragg peak (RSHB). Both indices also have a strong correlation with the underlying wave height. On the basis of all these indices an empirical model is proposed to estimate the wave height. This method has been used in a three-months long experiment of the ocean state measuring and analyzing radar, type S (OSMAR-S), which is a portable HFSWR with compact cross-loop/monopole receive antennas developed by Wuhan University since 2006. During the experiment in the Taiwan Strait, the significant wave height varied from 0 to 5 m. The significant wave heights estimated by the OSMAR-S correlate well with the data provided by the Oceanweather Inc. for comparison, with a correlation coefficient of 0.74 and a root mean square error (RMSE) of 0.77 m. The proposed method has made an effective improvement to the wave height estimation and thus a further step toward operational use of the OSMAR-S in the wave height extraction.

Key words: wave height, high frequency surface wave radar, field experiment, comparison, Taiwan Strait

Citation: Zhou Hao, Roarty Hugh, Wen Biyang. 2015. Wave height measurement in the Taiwan Strait with a portable high frequency surface wave radar. Acta Oceanologica Sinica, 34(1): 73–78, doi: 10.1007/s13131-015-0599-6

1 Introduction

The knowledge of sea waves is always needed in a wide range of human's applications from weather forecasting, ocean engineering for the design and operational safety of harbors, ships, and offshore structures, to coastal management including coastal stability and pollution. Because the sea waves influence so many processes and operations at sea, many technologies have been invented for measuring waves in different temporal and spatial scales (Chen et al., 2013; Wang et al., 2013). Buoys can provide direct and *in-situ* wave measurements with the highest accuracy and the smallest scales, while a satellite altimetry can provide measurements over an extremely large spatial extent with relatively low resolutions in both time and space. A high frequency surface wave radar (HFSWR) fills the gap between these two methods, which can provide low-cost wave measurements by remote sensing with a time resolution of a few tens of minutes and a spatial resolution of several kilometers. Owing to the great advantages in sea state monitoring, the HFSWR has been continuously receiving attention from several researchers (Barrick, 1972; Gill et al., 2006; Wyatt et al., 2009; Zhou et al., 2012; Wu et al., 2012) and been established and tested worldwide in various situations. Now it is widely accepted and also expected to play a more important role in a modern sea surveillance network, where different instruments based on different mechanisms work together to provide measurements that can meet the needs of various applications with a higher accuracy and a higher confidence level.

The prevailing method used for wave extraction from the high-frequency (HF) radar echoes is mainly based on the first- and second-order electromagnetic scatter theory founded by Barrick (1972). The Doppler spectrum from the sea surface is dominated by two strong first-order peaks due to the Bragg scattering effect. There are also weaker spectral continuums adjacent to them. The overall power of the second-order continuum is normalized by the energy in the first-order region to calculate the significant wave height (Barrick, 1977). This method has been validated by several field comparison experiments. In a majority of situations, say under not very high sea states, high correlations between measurements by the HFSWR and by *in-situ* buoys can be achieved. However, an external interference may frequently lead to large errors in the radar-derived wave height estimates, which is a major problem in HFSWR

Foundation item: The National Natural Science Foundation of China under contract No. 61371198; the National Special Program for Key Scientific Instrument and Equipment Development of China under contract No. 2013YQ160793; the Natural Science Foundation of Jiangsu Province of China under contract No. BK2012199.
*Corresponding author, E-mail: zhou.h@whu.edu.cn

operations. Moreover, the incorrect delineation of the first- and second-order spectral regions due to spectral spread and split is also a source of error, especially when the radar beam is not sufficiently narrow. So, some measures should be taken to decrease the error and increase the confidence level of the wave height estimate.

Owing to the low cost and ease of installation and maintenance, the HFSWR with a compact antenna array is often preferred to that with a large-aperture array. The ocean state measuring and analyzing radar type S (OSMAR-S) is a portable HFSWR developed by Wuhan University of China, aiming at providing sea surface current, wave and wind parameters. The capability of the OSMAR-S on large-area current field measurement has been verified in a series of field experiments (Wen et al., 2009; Zhou et al., 2012), but only average wave and wind parameters can be obtained on each range cell so far due to the insufficient directional resolution. Furthermore, the OSMAR-S is more susceptible to external interferences than large-aperture radars and has a lower accuracy of the wave estimate. The wave extraction algorithm and the specific wave processing settings of the radar software still need to be further tested and improved by more experiments under different sea conditions.

From January to April 2013, the OSMAR-S was operated in Zhangpu County, Fujian Province to fully test its performance on sea state measurement. The surface current, wave height, wave period, wind direction and wind speed in the Taiwan Strait were measured continuously. In this paper, we discuss the wave height estimation. During the experiment, the significant wave height in the Taiwan Strait varied from 0 to 5 m. Buoys were placed in the radar detection area but the data are unavailable for comparison now. So alternatively the wave height provided by a global wave model GROW2012 developed by the Oceanweather Inc. (Hope et al., 2013) is used as the "ground truth" data here. The conventional integration-based method performed well and captured every varying cycle of the wave successfully with the correlation coefficient being 0.67 and the root mean square error (RMSE) being 0.89 m. However, some outliers were measured due to the external interferences. To improve the wave estimate, two semiempirical models are proposed to calculate the significant wave height simultaneously. One uses the ratio of the maximum power in the second-order spectral continuum to that of the Bragg peak (RSCB), and the other uses the ratio of the power of the second harmonic peak to that of the Bragg peak (RSHB). Using the peak power only instead of the integration means only the strongest sea waves of particular wavelengths are involved but many other weaker waves are ignored. This will of course lead to some errors in the wave height estimate, but the errors due to incorrect delineation of the first- and second-order regions and the external interferences will be effectively decreased. To make a further improvement, all the three estimates by the models are combined together and then smoothed to give the final wave height estimate. The comparison results show that the correlation coefficient increases to 0.74 and the RMSE decreases to 0.77 m.

2 Method for wave height estimation

2.1 *Conventional method*

HF echoes from the sea surface are dominated by the first-order or Bragg scatter peaks. In the 1970s, Barrick (Barrick, 1972) derived the first- and second-order cross-section equations for narrow-beam HF radars, which established the theoretic basis for the wave extraction. He also proposed an efficient method to calculate the significant wave height via the ratio of the overall power in the second-order spectral region to that in the first-order region (Barrick, 1977), i.e.,

$$r_0 = \frac{\int_{\Omega_2} \sigma_2(\omega)/W(\omega)\mathrm{d}\omega}{\int_{\Omega_1} \sigma_1(\omega)\mathrm{d}\omega}, \tag{1}$$

$$H_{S,0} = \alpha_0 \frac{4\sqrt{2}}{k_0}(r_0)^{0.5}, \tag{2}$$

where $\omega=2\pi f$ is the circular Doppler frequency; σ_1 and σ_2 are the first- and second-order power spectral densities respectively; k_0 is the radar wavenumber; W is a dimensionless weighting function to eliminate the coupling coefficient of the double scatter; Ω_1 and Ω_2 indicate the first- and second-order spectral regions respectively; and α_0 is a calibration factor. Usually only the spectral side with stronger Bragg peaks is involved in the above integrations. Till now this method has been used in most of the oceanographic radars.

As can be seen from Eqs (1) and (2), the delineation of the first- and second-order spectral regions has a crucial impact on the wave extraction, but often there is no clear null between them. If some first-order peaks are mistakenly included into the second-order spectrum, the wave height will be greatly overestimated. Moreover, because the second-order spectral continuums are relatively weak, even a moderate interference or clutter can lead to a significant rise in the wave height estimate.

2.2 *Semiempirical method I*

To account for the susceptibility to the noise and difficulty in allocating the spectral regions, more indices may be included in the wave height estimation. Intuitively, the ratio of the maximum value of the second-order continuum to that of the first-order region may be such a helpful index. The second-order peak region contains a large portion of the total power of the wave height spectrum, and usually it is much easier to locate the second-order peak only than to determine the edges of the first- and second-order spectral regions. Moreover, when there exist interferences, the delineation of the spectral regions is more likely to be affected, and thus larger error may result. In fact, there is a quantitative relation between the integration and the peak value of the wave height spectrum for some particular wave models. Here we consider the two most popular spectral models, i.e., the Pierson-Moskowitz (P-M) spectrum (Pierson and Moskowitz, 1964) for a fully developed sea and the Joint North Sea Wave Project (JONSWAP) spectrum (Hasselmann et al., 1980) for a not fully developed sea. The JONSWAP spectrum is given by

$$S(\omega) = \frac{\alpha g^2}{\omega^5}\exp\left(-\beta\frac{\omega_\mathrm{p}^4}{\omega^4}\right)\gamma^a, \tag{3}$$

where

α=0.008 1; g=9.8 m/s^2; β=1.251; $a=\exp[-(\omega-\omega_\mathrm{p})^2/2\omega_\mathrm{p}^2\sigma^2]$, with

$$\sigma = \begin{cases} 0.07 & \omega \leqslant \omega_\mathrm{p} \\ 0.09 & \omega > \omega_\mathrm{p} \end{cases},$$

in which $\omega_\mathrm{p}=2\pi f_\mathrm{p}$, is the peak circular frequency; and γ is a peak enhancement parameter between 1 and 7.

The power of the P-M spectrum, E, can be expressed by

$$E=\int_0^{\infty} S(\omega)\,\mathrm{d}\,\omega=\frac{\alpha g^2}{5\omega_{\mathrm{p}}^4}, \tag{4}$$

and the peak value is given by

$$S(\omega_{\mathrm{p}})=\frac{\alpha g^2}{\omega_{\mathrm{p}}^5}\mathrm{e}^{-\beta}. \tag{5}$$

The ratio of the overall integration to the modified peak value (RIP) is

$$k_1=\frac{E}{[S(\omega_{\mathrm{p}})]^{0.8}}=0.2(\alpha g^2)^{0.2}\mathrm{e}=0.517. \tag{6}$$

The power of the JONSWAP spectrum has no analytical expressions available but can be calculated numerically. The RIP in the JONSWAP spectrum with a given γ is also nearly a constant

$$k(\gamma)=\frac{E(\gamma)}{[S(\omega_{\mathrm{p}})]^{0.8}}, \tag{7}$$

which is shown in Fig. 1 for different γ from 1 to 7.

So, with the nearly definite relationship between the overall integration and the peak value of the JONSWAP spectrum, the semi-empirical index based on the ratio of the maximum of the second-order continuum to the Bragg peak power (RSCB) for the wave height estimation can be denoted as

$$r_1=\left\{\frac{\max[\sigma_2(\omega)]}{\max[\sigma_1(\omega)]}\right\}^{0.8}, \tag{8}$$

$$H_{S,1}=\alpha_1(r_1)^{0.5}, \tag{9}$$

with α_1 being a calibration factor to be determined by fitting to the data.

2.3 *Semiempirical method II*

From a large amount of the HFSWR data, we find the ratio of the power of the second harmonic peak to that of the Bragg peak (RSHB) can also be used to estimate wave heights. The second harmonic peak is a line spectrum within the second-order spectral region which is located at $\sqrt{2}$ times Bragg frequency. This peak corresponds to a singularity in Barrick's (1972) second-order integral equation. It is due to both electromagnetic and hydrodynamic second-order effects. The electromagnetic effect is from ocean waves of length being equal to the radar wavelength, and the hydrodynamic effect is from a second spatial harmonic of the same wavelength. In the conventional method as described in Eqs (1) and (2) the second harmonic peak is weakened by setting small weights at the specific frequency position. Some research has been performed to quantitatively explain the second harmonic peak in the HF radar spectra. Ivonin et al. (2006) derived a quantitative expression of the second harmonic peak in the HF radar spectra and showed that the second harmonic peak was primarily due to the water wave of wavelength being equal to the radar wavelength λ_0, or twice that of the Bragg wave. By the boundary perturbation method, Zhang et al. (2013) derived a different form of the second harmonic peak. However, the evaluations of these theoretical models show that they do not correlate with the experimental results well. Because the second harmonic peak has a similar spectral structure as the Bragg peak and often has a strong strength, the use of it in the wave height estimation will certainly be helpful due to the reduced complexity, extra confidence level and improved accuracy.

The RSHB-based semi-empirical method to estimate the wave height can be described as

$$r_2=10\lg\left\{\frac{\max[\sigma_2(\sqrt{2}\omega_{\mathrm{B}}+\omega_{\mathrm{C}}+\Delta)]}{\sigma_1(\omega_{\mathrm{B}}+\omega_{\mathrm{C}})}\right\}, \tag{10}$$

$$h=\alpha_2 r_2+\beta_2, \tag{11}$$

$$H_{S,2}=\begin{cases}h & \text{when } h>0\\ 0 & \text{when } h\leqslant 0\end{cases}, \tag{12}$$

where $\omega_{\mathrm{B}}=\sqrt{2gk_0}$, is the circular Bragg frequency; ω_{c} is the circular Doppler frequency shift due to the underlying radial current velocity; Δ is a small neighborhood of the predicted position for the second harmonic peak to account for the underlying current shear; and α_2 and β_2 are the linear model parameters to be determined by fitting to the data. In this paper, Δ is empirically set to be within three frequency bins.

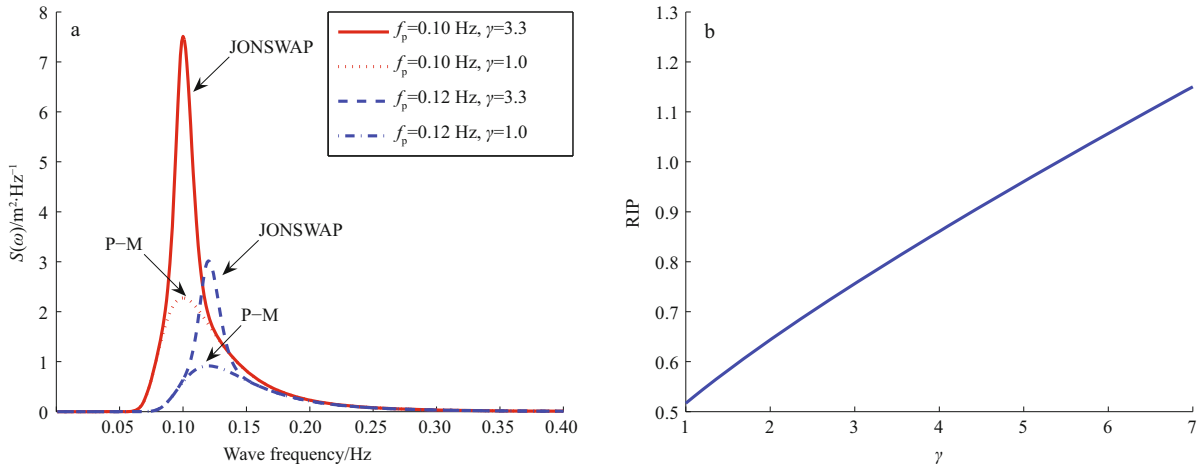

Fig. 1. The JONSWAP spectrum (a) and the RIP of the JONSWAP spectrum versus parameter γ (b).

2.4 *Combination and postprocessing*

Each model by itself may be susceptible to some kind of external noise. However, it can be expected that a combination or fusion of all the three wave estimates will effectively decrease the error. The combined wave height estimate can be denoted as

$$H_S = \sum_{i=0,1,2} w_i H_{S,i}, \tag{13}$$

where w_i (i=0, 1, 2) is the positive weights satisfying $\sum_{i=0,1,2} w_i = 1$.

To make a further improvement, smoothing is performed on the wave height sequence to give the final result with 1 h time step.

3 Description of radar experiment

The field experiment of the OSMAR-S was performed on the western coast of the Taiwan Strait from January 10 to March 31, 2013. During the experiment, the wind predominantly blew from the northeast direction with a speed varying from 0 to more than 20 m/s, and the wave height varied from 0 to above 6 m. The observation system consisted of two radar sites working near the 13 MHz band, namely XIAN (23°44.60′N, 117°36.29′E) and SHLI (24°9.85′N, 117°59.01′E), both located in Zhangpu County of Fujian Province. The geographic map is shown in Fig. 2. The radial current maps provided by the two radar sites were combined to calculate the corresponding vector current map, while each radar site independently provided the wave and wind estimates of its adjacent sea area. The sea state parameters were output every 20 min, and 3-months long continuous data were obtained. The system parameters of the OSMAR-S used in the experiment are listed in Table 1 for brevity. During the experiment, the external noise level at SHLI had been at least 6 dB higher than that at XIAN, so hereinafter only the wave height output from XIAN is to be discussed. Figure 3 shows a Doppler spectrum collected by XIAN for example, where the ratio of Bragg peak to noise power has exceeded 40 dB showing a high signal quality.

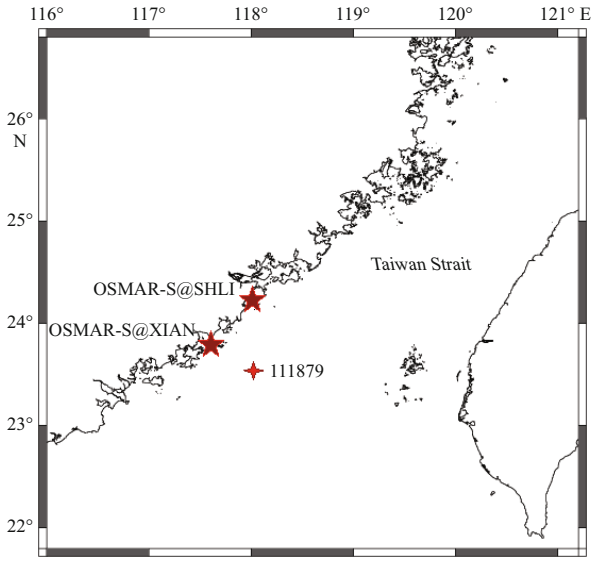

Fig. 2. Geographic map of the radar experiment 2013 in the Taiwan Strait. The pentagram marks the XIAN radar site and the four-pointed star indicates the grid point No. 111879 in the GROW2012 project developed by the Oceanweather Inc.

Table 1. System parameters of OSMAR-S used in the experiment

Center frequency/MHz	13±0.4
Waveform	frequency modulated interrupted continuous wave (FMICW)
Band width/kHz	60
Average power/W	100
Transmit antenna	monopole
Receive antenna	cross-loop/monopole
Sweep period/s	0.38
Coherent processing time/min	20

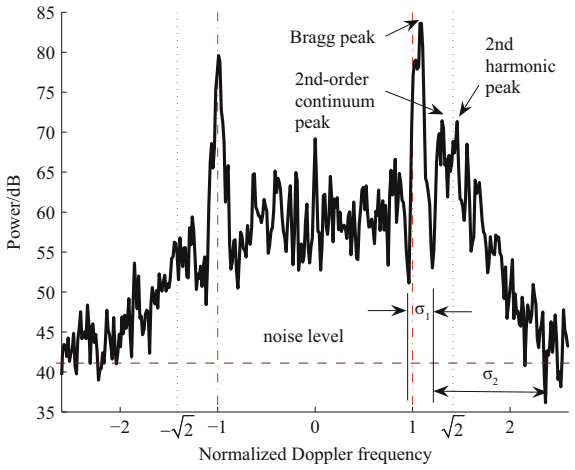

Fig. 3. Doppler spectrum collected by OSMAR-S at XIAN at 08:15, February 8, 2013. The range is 10 km. The Bragg region σ_1 and the second continuum region σ_2 in the conventional method are indicated.

Till now, there is no *in-situ* buoy data available for comparison, but the wave parameters output from GROW2012 (global reanalysis of ocean waves, 2012) developed by the Oceanweather Inc. can be used as the "ground truth" data. The GROW2012 couples Oceanweather's global wave model, tropical boundary layer model, and its vast experience in developing marine surface wind fields to produce a global wave hindcast. The wave output is available at an hourly time step on a 55 km grid. In consideration of the coverage of the XIAN site, grid point No. 111879 (23°30′N, 118°00′E) is most suitable for comparison, which is about 48 km far from the radar as indicated by a four-pointed star in Fig. 2.

4 Comparison results

The significant wave height estimates are calculated by the conventional integration-based method and the two line-spectrum-based semi-empirical methods at a range cell of 10 km in the direction of the grid point where comparison data are available. By fitting to the wave height sequence provided by the Oceanweather Inc, the parameters in the models are determined to be α_0=1.26, α_1=14.0, α_2=0.4 and β_2=10.0, respectively. The three wave height estimates by the OSMAR-S are shown in Fig. 4, with the wave height provided by the Oceanweather Inc. for comparison. As can be seen, all the three methods have tracked the variations of the wave height generally well. There are several outliers in the results by the conventional method due to external interferences, whereas there are less by the

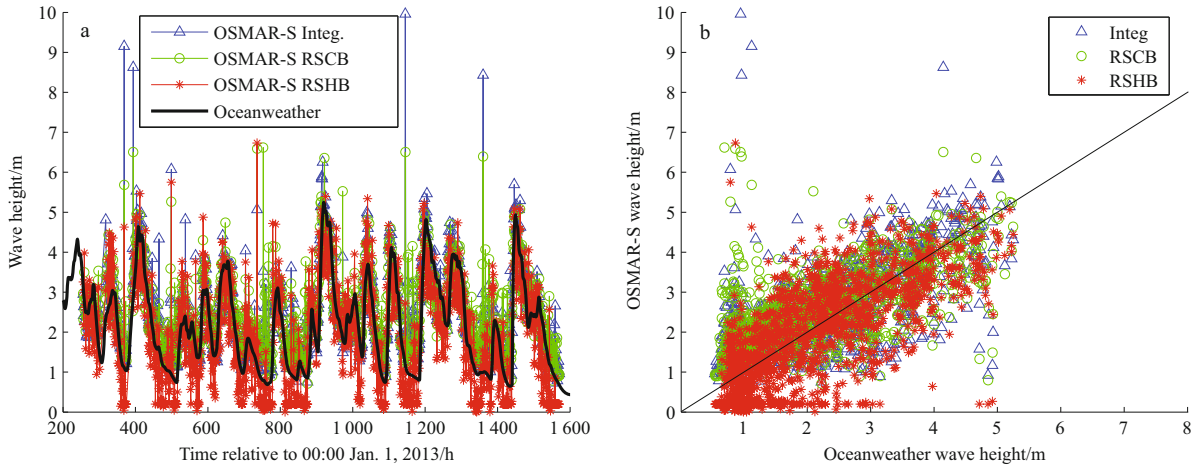

Fig. 4. Comparisons of the significant wave height estimates by the conventional method and the semi-empirical methods versus that provided by the Oceanweather Inc. a. The time sequences and b. the scatter plots.

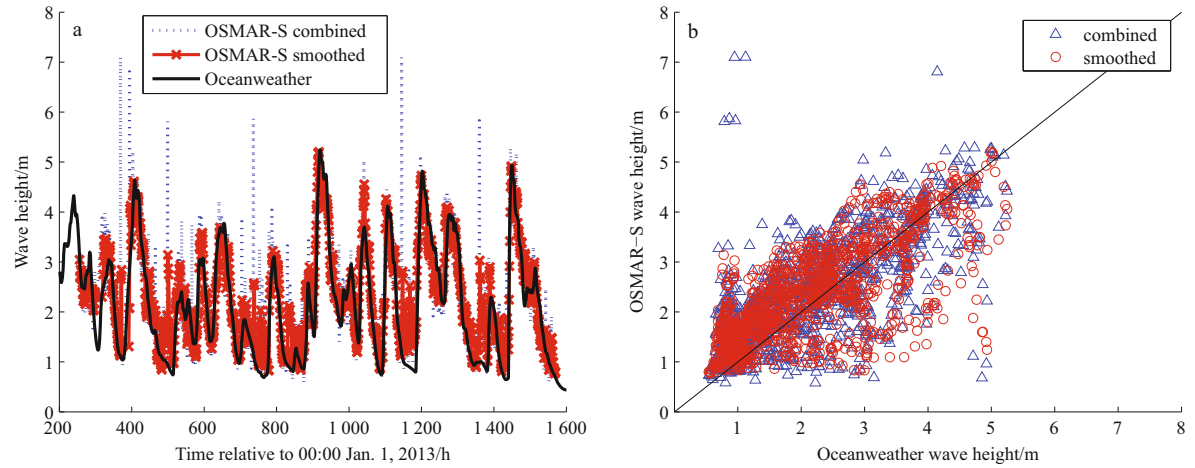

Fig. 5. Combined and smoothed significant wave height estimates by the OSMAR-S versus that provided by the Oceanweather Inc. a. The time sequences and b. the scatter plots.

RSCB-based method and the least by the RSHB-based method. Then these three wave height estimates are combined and smoothed using a 1 h moving window to give the final result, as shown in Fig. 5. The weights used here are w_1=0.5, w_2=0.2 and w_3=0.3, respectively, corresponding to the different priorities of the three indices used here. As can be seen, the wild values have been removed and the fluctuations in the intermediate wave height estimates have been greatly reduced.

The correlation coefficients and the RMSE between the wave height estimates by the OSMAR-S and that by the Oceanweather Inc. are shown in Table 2. It can be seen that the three methods generally have similar statistics, with the RSHB-based method giving the highest correlation but the biggest error while the RSCB-based method gave the lowest correlation but also the smallest error. The combination of the three estimates and the further smoothing have effectively improved the wave height estimate, which makes the wave estimate more acceptable towards operational use.

Table 2. Correlation coefficients and standard error between the estimates by the OSMAR-S and the estimates by the Oceanweather Inc.

Method	Correlation coefficient	RMSE/m
Integration-based	0.67	0.89
RSCB-based	0.65	0.87
RSHB-based	0.71	0.93
Combined	0.72	0.82
Smoothed after combination	0.74	0.77

5 Conclusions

The wave height is one of the most important dynamic parameters of the sea. The conventional method for the wave height estimation in HFSWR involves the integrations of the first- and second-order Doppler spectra. There are two major sources of large errors in the wave estimates, especially for the portable radar like the OSMAR-S with a compact antenna array. One is the strong external noise received by the HFSWR, and the other is the incorrect delineation of the first- and second-order spectral regions. To achieve higher accuracy and confidence level in the wave measurement, two more indices, namely the RSCB and the RSHB, are incorporated into the wave estimation. The linear models are used and the parameters are determined by fitting the ratios to the ground truth wave heights. Calcula-

tions show that these new indices lead to similar correlation coefficients and estimation errors as the conventional integration-based method. But the combination of all the three indices can effectively improve the estimates. This processing has advanced toward the operational use of the wave estimation by a portable HFSWR.

Till now the theoretical relations between the new indices and the underlying wave height have not been fully developed, and the above new models used for the wave height estimation are currently semi-empirical. Our future work will include more theoretical analyses of these indices, further improving the signal quality by more sophisticated signal processing technologies, and doing more experiments to test and improve the methods.

Acknowledgements

The authors would like to thank the personnel of the Wuhan Devices Electronic Technology Co, Ltd. for their endeavor to accomplish the field experiment.

References

Barrick D E. 1972. Remote sensing of the sea state by radar. In: Derr V E, ed. NOAA/Environ Mental Research Laboratories, Remote Sensing of the Troposphere. Vol. 12. Washington, DC: U.S. Government Printing Office, 1–46

Barrick D E. 1977. Extraction of wave parameters from measured HF radar sea-echo Doppler spectra. Radio Science, 12(3): 415–424

Chen Chuntao, Zhu Jianhua, Lin Mingsen, et al. 2013. The validation of the significant wave height product of HY-2 altimeter-primary results. Acta Oceanologica Sinica, 32(11): 82–86

Gill E, Huang W, Walsh J. 2006. On the development of a second-order bistatic radar cross section of the ocean surface: a high-frequency result for a finite scattering patch. IEEE Journal of Oceanic Engineering, 31(4): 740–750

Hasselmann D E, Dunckel M, Ewing J A. 1980. Directional wave spectra observed during JONSWAP 1973. Journal of Physical Oceanography, 10(8): 1264–1280

Hope M E, Westerink J J, Kennedy A B, et al. 2013. Hindcast and validation of Hurricane Ike (2008) waves, forerunner, and storm surge. Journal of Geophysical Research: Oceans, 118(9): 4424–4460

Ivonin D V, Shrira V I, Broche P. 2006. On the singular nature of the second-order peaks in HF radar sea echo. IEEE Journal of Oceanic Engineering, 31(4): 751–767

Pierson W J Jr, Moskowitz L. 1964. A proposed spectral form for fully developed wind seas based on the similarity theory of S. A. Kitaigorodskii. Journal of Geophysical Research, 69(24): 5181–5190

Wang Jichao, Zhang Jie, Yang Jungang. 2013. The validation of HY-2 altimeter measurements of a significant wave height based on buoy data. Acta Oceanologica Sinica, 32(11): 87–90

Wen Biyang, Li Zili, Zhou Hao, et al. 2009. Sea surface currents detection at the Eastern China Sea by HF ground wave radar OSMAR-S. Acta Electronica Sinica (in Chinese), 37(12): 2778–2782

Wu Xiongbin, Li Lun, Li Yan, et al. 2012. Experimental research on significant waveheight detecting with HFSWR OSMAR071. Oceanologia et Limnologia Sinica (in Chinese), 43(2): 210–216

Wyatt L R, Green J, Middleditch A. 2009. Signal sampling impacts on HF radar wave measurement. Journal of Atmospheric and Oceanic Technology, 26(4): 793–805

Zhang Shoushou, Wen Biyang, Zhou Hao. 2013. Analysis of the higher order Bragg scatter in HF radar. Journal of Electromagnetic Waves and Applications, 27(4): 507–517

Zhou Hao, Wen Biyang, Wu Shicai, et al. 2012. Sea states observation with a portable HFSWR during the 16th Asian Games Sailing Competition. Chinese Journal of Radio Science (in Chinese), 27(2): 293–300